Available online at www.sciencedirect.com
SCIENCE DIRECT®
ELSEVIER
International Journal of Multiphase Flow 31 (2005) 771–792
International Journal of Multiphase Flow
www.elsevier.com/locate/ijmulflow

Air–water counter-current slug flow data in vertical-to-horizontal pipes containing orifice type obstructions

A. Teyssedou [a,*], E.N. Önder [a], P. Tye [b]

[a] *Nuclear Engineering Institute, Engineering Physics Department, École Polytechnique, P.O. Box 6079, succ., Centre-ville, Montréal, Qué., Canada H3C 3A7*
[b] *Brais, Malouin and Associates, Inc., 5450 Côte-des-Neiges Suite 600, Montréal, Qué., Canada H3T 1Y6*

Received 28 December 2003; received in revised form 23 March 2005

Abstract

This paper presents experimental counter-current air–water flow data on the onset of flooding and slugging, the slug propagation velocity, the predominant slug frequency and the average void fraction collected by using different size orifices installed at two locations in a horizontal pipe. For the flow conditions covered during these experiments, it was observed that there is no significant difference between the onset of flooding and the onset of slugging when an orifice is installed in the horizontal run. However, a difference was observed for the experiments carried out without orifices. Furthermore, the position of the orifice with respect to the elbow does not affect the onset of flooding and slugging. When an orifice is installed in the horizontal run, it was observed that slugs occur due to the mutual interaction (constructive interference) of two waves traveling in opposite directions. This means that a completely different mechanism seems to govern the formation of slugs in counter-current two-phase flows in horizontal partially blocked pipes. This is in contrast to that described for the slugging phenomena in co-current flow, where wave instability seems to be the principal mechanisms responsible of bridging the pipe. The mutual interaction of waves traveling in opposite directions seems to control the behaviour of the slug propagation velocity, the slug frequency and average void fraction with increasing the gas superficial velocity.

Keywords: Slugging; Slug frequency; Slug propagation velocity; Counter-current two-phase flow; Flow obstructions

* Corresponding author.
E-mail address: alberto.teyssedou@polymtl.ca (A. Teyssedou).

0301-9322/$ - see front matter
doi:10.1016/j.ijmultiphaseflow.2005.03.005

1. Introduction

In CANDU nuclear power reactors the horizontal fuel channels are connected to inlet and outlet headers by feeder-pipes. These pipes consist of vertical and horizontal legs; in some feeders, orifices and/or venturi type flow obstructions are installed for flow adjustments and measurements. During some postulated loss of coolant accidents (LOCA), the emergency cooling water injected into the inlet and outlet headers enters the fuel channels through the feeder pipes. Steam produced in the feeders and/or in the fuel channels, which under depressurization can be at a temperature higher than saturation, may flow in the direction opposite to that of the water, thereby creating vertical and horizontal counter-current flow (CCF). Under these conditions, the rate at which the cooling water enters the fuel channel may be substantially limited by the flooding phenomena. Starting at the flooding point, the water is partly entrained in the same direction as the steam flow. Under these conditions, the steam produced in the feeders and/or in the fuel channels flowing in the direction opposite to the emergency cooling water can bring about the formation of slug flow. Thus, long slugs of liquid moving at relatively high speed are transported back towards the headers by the steam. This substantially reduces the amount of cooling water that can reach the reactor core. Therefore, understanding the slugging phenomena in vertical-to-horizontal pipes under counter-current two-phase flow conditions may help to better predict the emergency cooling conditions for nuclear power reactors.

Most of the research carried out using vertical to horizontal or inclined pipes have been essentially devoted to study the effect of pipe orientation, pipe inside diameter (ID) and length on the flooding conditions. These kinds of problems were studied by among others Krowlewski (1980), Siddiqui et al. (1986), Wan and Krishnan (1986), Ardron and Banerjee (1986) and Kawaji et al. (1989). In all cases it was observed that there is a significant decrease in the superficial gas velocity required to provoke flooding as compared to that which is required for the same tube ID under vertical flow conditions. It has been also reported that the inclination of the pipe with respect to a horizontal plane strongly affects the onset of flooding.

None of the aforementioned studies looked at the effect of obstructions on CCF and counter-current flooding limit (CCFL). To the best of the author's knowledge, up to now only a few researchers have studied this problem. Celata et al. (1989) performed flooding and pressure drop experiments with air–water counter-current flows in a vertical 200 mm ID 500 mm long circular test section. Orifices of different diameters ranging from 12 to 19 mm were placed concentrically in the test section 300 mm downstream from the liquid entrance. Tests were also carried out with four non-concentric orifices. The flooding point was defined as a point at which the falling film began to be entrained by the gas. It was found that the superficial gas velocity at the onset of flooding decreases with decreasing orifice perforation ratio defined as, $\mathscr{P} = \text{Orifice area}/\text{Pipe area}$.

Kawaji et al. (1993) carried out experiments to determine the CCFL in a 51 mm ID test section with multiple elbows and orifices having β ratios ($=D_{\text{orif}}/D_{\text{tube}}$) of 0.55, 0.670, and 0.885. Three different geometrical configurations were studied: double-vertical elbow in which the second and third elbow are in the vertical plane; double-horizontal elbow in which the second and third elbow are in the horizontal plane, and double-inclined elbow in which the second and third elbow are at 45° to the vertical plane. Although there are some differences in the results for the three different geometries studied, general observations can be made as to the effects of the orifice size on the flooding point. The authors found that the orifice having the largest β ratio has very little effect on the flooding point as compared to the results without the orifice. For the two smaller orifices, it was found that for a given liquid flow rate, the flooding gas velocities are much smaller than those observed with the largest orifice and no orifice case. Further, the flooding gas velocity was found to decrease with decreasing orifice β ratio. Tye (1997) and Tye and Teyssedou (2000) studied both the effect of different orifice sizes as well as their position with respect to an elbow on flooding for vertical to horizontal CCF. They carried out the experiments by using the same facility that has been used to carry out the present work. Similarly to Kawaji et al., Tye and Teyssedou found that the onset of flooding is strongly affected by the size of the orifice, i.e., the superficial gas velocity required to trigger flooding decreases with decreasing the orifice β ratio. In addition, they also found that the flooding conditions are not affected by the position of the orifice with respect to the elbow. They compared the flooding data with the data of Kawaji et al.; in the region where Kawaji et al. reported that the flooding occurred as a result of the presence of the orifice; a good agreement between the data was observed.

As mentioned above, studies carried out on the characterization of slug flow under counter-current two-phase flow conditions in pipes containing singularities are very scarce or non-existent. Most of the studies on two-phase slug flows have been carried out with the two phases flowing co-currently. Wallis and Dobson (1973) conducted co-current as well as counter-current two-phase slug flow experiments under conditions of flowing and stagnant water in a horizontal rectangular channel. They observed that slugging could be triggered both; by increasing the air or the water superficial velocities or by changing the slope that the pipe forms with the horizontal plane. Once slugging was initiated, the delivered liquid flow rate in the channel was substantially reduced with most of the water being carried over by the gas phase. They also found that the transition from stratified to slug or plug flow in a horizontal pipe occurred at a critical value of the relative velocity between the phases which is given by, ($u_g - u_l = 0.5[gh_g(\rho_l - \rho_g)/\rho_g]^{1/2}$). Johnston (1985) carried out experiments using Kerosene and a zinc chloride solution as working fluids flowing counter-currently. He used three different diameter pipes (0.057, 0.069 and 0.095 m) with inclinations ranging from 0° to 18° with respect to the horizontal plane. The data was analyzed by using a stability criterion based on the growth and collapse of interfacial waves, i.e., Kelvin–Helmholtz instability criterion (Taitel and Dukler, 1976). Johnston concluded that it is possible to predict the transition from stratified to slug flow in counter-current flow by using such a stability criterion.

One of the first mechanistic two-phase slug models for co-current flows was given in Dukler and Hubbard (1975). To develop their model, Dukler and Hubbard considered that the liquid phase was scooped up at the slug front, accelerated up to the slug velocity and then passed back through the slug. Although the model provides a good understanding of the mechanisms that govern the formation of the slugs, it requires several empirical parameters in order to be useful for practical calculations. Taitel and Dukler (1977) proposed a model to predict the slug frequency in co-current two-phase flows by considering that the slug formation was essentially controlled by entry region effects. They found that the proposed theoretical approach was able to predict the slug frequency only when the slugs were formed at the entrance section of a stratified flow, otherwise the model failed in predicting the slug frequency. Crowley et al. (1992) used one-dimensional wave theory to predict the transition from stratified to slug flow using a criterion based on the instability caused by an overtaking process of continuity waves (v_w) over dynamic waves (c). In their work, the instability criterion was expressed by the inequality between the square of these velocities, i.e., $v_w^2 > c^2$.

Despite all these studies, the physical mechanisms that govern the slugging phenomena have yet to be properly understood. Furthermore, to the best of the authors' knowledge, there is no experimental information in the open literature concerning studies on counter-current slug flow in vertical-to-horizontal pipes containing flow obstructions. Thus, the purpose of this paper is to provide data to characterize slug flow occurring due to the hydrodynamic interaction between an elbow and an orifice located in a horizontal pipe.

2. Experimental facility

The CCF test facility is shown in the insert of Fig. 1. This system consists of a constant head water tank, a pump, a calming section, a bank of water turbine-type flow meters and air rotameters and the test section. The water flow rate, supplied to the test section by the pump connected

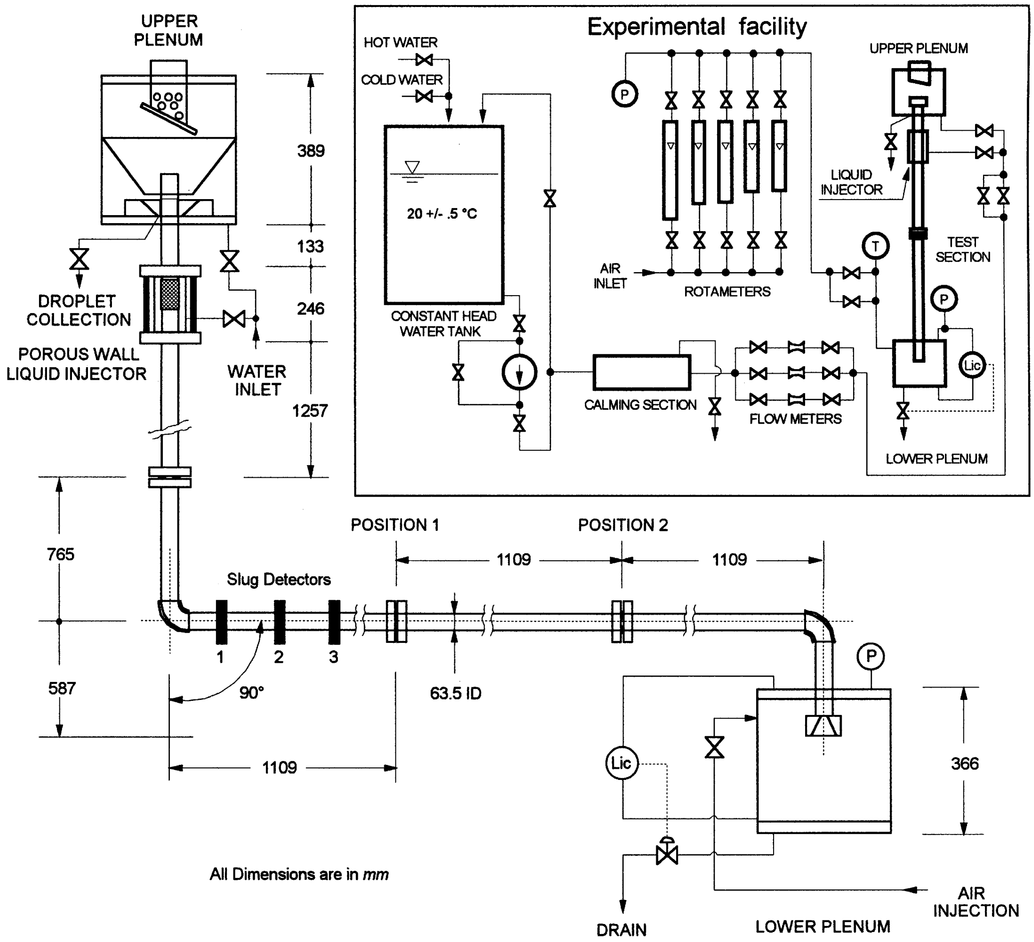

Fig. 1. The experimental facility and the test section.

to the constant head water tank, is controlled in two steps: a coarse control that is done using a set of valves and a by-pass circuit at the pump outlet, and a fine control that is done using a set of two different size parallel needle valves located close to the test section. During the experiments the temperature of the water is kept constant at 20 ± 0.5 °C.

2.1. The test section

The schematic of the test section is shown in Fig. 1. The major components of the test section are: the upper and a lower plenum, the vertical and horizontal legs connected by elbows and the orifices. The upper plenum is used as a collector/separator for any liquid hold up during CCF and CCFL experiments. The porous wall liquid injector consists of a 63.5 mm ID tube with 800, 1 mm holes in the wall. The test section, that has a geometry similar to a typical feeder pipe encountered in CANDU nuclear power reactors, consists of 2.02 m long vertical and 3.30 m long horizontal legs. The horizontal leg contains flanges in which an orifice may be placed. The vertical and horizontal legs are connected by an opaque 90° PVC elbow. These legs are centered in the elbow by two Plexiglas collars and are sealed using O-rings. In order to allow flow visualization, both the vertical and the horizontal legs are manufactured from 63.5 mm ID transparent Plexiglas tubes. The lower plenum contains the liquid outlet including a water level control system and the air inlet system. The level control consists of a 0.34 bar differential pressure transducer used as liquid level transducer. The signal produced by this transducer is used as the process variable input of an electronic level controller developed in house. The level control system is capable of maintaining the water level in the lower plenum constant ($\approx\pm1$ cm) through a wide range of superficial liquid velocities, i.e., from full liquid delivery up to the zero liquid penetration point. The orifices are made of 3 mm thick stainless steel plates without a chamfered edge and are coaxial with the pipe. The β ratios of the orifices used in these experiments are 0.66, 0.72, 0.77 and 0.83.

2.2. Instrumentation

The test section is instrumented to measure liquid and gas flow rates, inlet flow temperatures, absolute pressures, and void fractions. The liquid flow rate is measured using ‘‘Flow Technology’’ turbine flow meters covering a range of 0.05–4.54 m^3/h having an accuracy better than 1% of the reading. The gas flow rate is measured using a set of five ‘‘Brooks’’ rotameters, covering a range of 0.085–132.5 m^3/h $\pm 2\%$ of full scale, at an outlet absolute pressure of 2 bara. The temperature of the air is measured using a K-type thermocouple installed near the air entrance to the lower plenum. The absolute pressure in the lower plenum is measured using a 1.4 bara ‘‘Sensotec’’ pressure transducer with an accuracy of 0.25% of full scale. The void fraction measurement system, also used as the slug detection system consists of three mobile capacitance probes (Teyssedou and Tye, 1999). Each probe consists of two electrodes manufactured using a 0.06 mm thick metallic foil deposited on a Plexiglas collar; the topology of these probes is shown in Fig. 2. It is important to note that with the proposed arrangement of the electrodes one of them is connected to ground and is simultaneously used as a Faraday electrostatic shield for the second one. Each void probe with its associated electronics module and anti-alias filters was calibrated under steady state conditions. For the calibration a small test section 0.15 m in length, with the same ID, wall thickness, and material (Plexiglas) as that used for the CCF test section shown in Fig. 1 where the probes

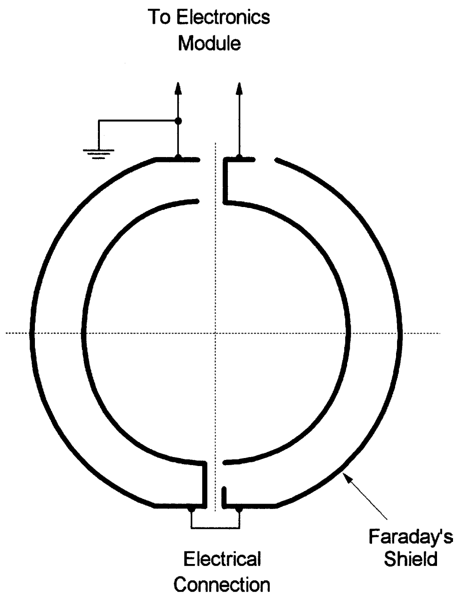

Fig. 2. Topology of the void probe electrodes.

were finally installed, was used. With the optimization of the geometry of the electrodes used for each probe it was possible to obtain an almost linear response of the apparatus for void fractions of up to 70%. The accuracy of this instrument was determined to be better than 5% of the readings and the time response of each probe was better than 1×10^4 V/s. Since the capacitance of the electrodes is quite low (few μμF) and the inductance of the electrical connections is very low, the time response is only limited by the anti-alias filter integrated in the electronic modules. The position of the probes installed in the horizontal leg with respect to the elbow is shown in Fig. 1. The distance of the first probe with respect to the elbow is maintained constant at 0.19 m while the distance between probes 2 and 3 with respect to probe 1 is varied from 0.20 to 0.40 m. The output of these modules as well as the output of the pressure transducer located in the lower plenum are connected to a data acquisition system (DAS). The DAS has a 16-bit analog to digital conversion unit, and is connected to a PC. The DAS is capable of collecting 66000 data points (13200×5 channels) per run with a sampling time of 20 ms. In order to minimize the amount of data and to avoid aliasing of the signals, the sampling time was selected after a careful analysis of the void signals using a HP spectrum analyzer.

3. Experimental conditions and procedures

In the past, several different physical phenomena have been used to determine the flooding point and consequently the CCFL. Some authors identified it with liquid bridging, surface wave instabilities, inception of droplet entrainment, etc. None of these phenomena necessarily leads to a net upward liquid flow. The liquid that is entrained above the liquid inlet may subsequently flow downward. In general, three main criteria have been used by different authors for the characterization of the CCFLs (Tien et al., 1979): (a) point of inception of liquid entrainment; (b) inception, of liquid film up flow and (c) zero liquid penetration. It is important to mention that for a given superficial liquid velocity these events can occur at significantly different superficial gas velocities. The standard definition of the CCFL and the one used in this work is (Bankoff and Lee, 1986): "for a given downward liquid flow the maximum upward gas flow rate which full liquid delivery out the bottom of the tube is maintained, corresponds to the counter-current flooding limit". Thus, the CCFL is just a limit for the superficial gas velocity beyond which only partial liquid delivery out of the lower plenum will occur. This point corresponds to the maximum superficial gas velocity for which full liquid delivery still exists.

In order to apply the criterion given above, the inlet liquid flow rate and the liquid delivery were measured simultaneously. Thus, for a given orifice size ($\beta = 0.66, 0.72, 0.77$ and 0.83) and position in the horizontal leg, and a given superficial liquid velocity, the superficial gas velocity was slowly increased up to the moment that a difference between the inlet and delivered liquid flow rates was observed. These flow conditions were considered as the point of onset of flooding. Simultaneously, the visual observation of the flow in conjunction with the void fraction signals produced by the slug detector probes, permitted the onset of slugging in the horizontal leg to be determined. After reaching the onset of flooding and slugging conditions, the superficial gas velocity was increased in order to cover the entire partial liquid delivery region. Furthermore, for each orifice the experiments were repeated for superficial liquid velocities ranging from 0.035 to 0.22 m/s.

For each pair of liquid and gas superficial velocities, the signals produced by three slug detector probes as well as the signal produced by the pressure transducer used to measure the absolute pressure in the lower plenum were collected simultaneously. After having finished the experiments, these signals were post processed using a program developed in house that allows the Fast Fourier Transform (FFT), the mean value of the void fraction and pressure signals, the probability density function (PDF) and the cross-correlation of the signals to be determined. The calibration curve of the void probes in conjunction with the normalized response of each probe are used to determine the average void fraction at different locations in the horizontal run. Cross-correlating the time series between different void probes in conjunction with the distance between the probes are used to determine the most probable slug propagation velocity for a given experimental condition.

The capability of the hardware and software used to collect and treat the data was determined according to the following procedure. A function generator was connected to one of the channels of the DAS. Sinusoidal signals covering a range of 0.2–5.0 Hz and having a constant amplitude of 4 V were applied to one of the DAS channels and collected with a sampling rate of 20 ms. A two channel "Gould" digital oscilloscope (100 Ms/s) and a "Fluke" frequency counter were simultaneously used to monitor the incoming signals to the DAS. The probability density functions of the void signals followed almost a Gaussian distribution. Therefore, the collected sinusoidal signals were then numerically mixed with a Gaussian noise having a similar distribution function as the void fraction signals. Fig. 3 shows the distribution function of a void fraction signal collected during an experiment carried out using an orifice having a β ratio of 0.77 installed at Position 1 in the horizontal leg (see Fig. 1). The mixed signals were then treated by the FFT software and the intensity of the noise was subsequently increased up to a level that the fundamental frequency of the sinusoidal signal was not able to be detected by the FFT processor. Fig. 3 also shows the distribution function of a 0.2 Hz sinusoidal signal after being mixed with a Gaussian noise having an

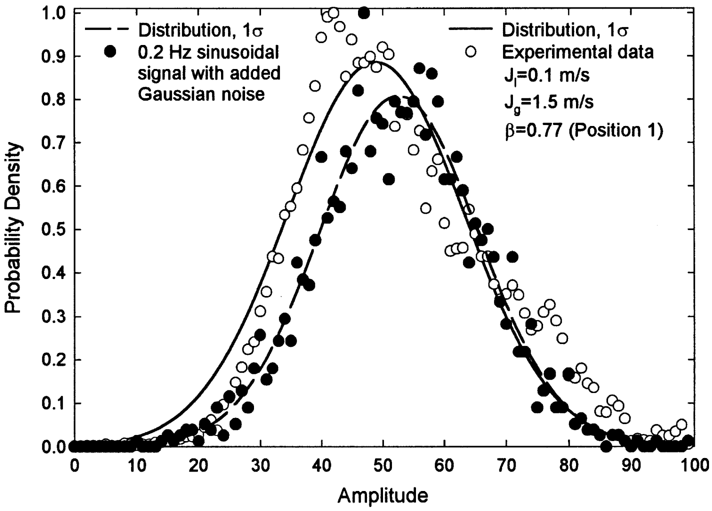

Fig. 3. Distribution functions.

amplitude of 30 V. This noise amplitude represents the upper limit where the peak of the fundamental frequency produced by the signal generator can still be detected. Under this limiting condition it was determined that the signal to noise ratio (SNR) of the technique used to treat the data, is approximately 18 dB ($=20\log(30/4)$; for a constant and the same coupling impedance). The spectra of both the void fraction and pressure signals obtained from the same experiment, i.e., $\beta = 0.77$, $J_l = 0.1$ m/s and $J_g = 1.5$ m/s, are shown in Fig. 4. Even though there is a long distance between the void probes and the pressure transducer installed in the lower plenum (≈3 m in Fig. 1), it is interesting to note the similarity that exists in the frequency components of these two signals. In both cases the predominant frequency of the slugs is close to 0.2 Hz.

4. Experimental results

Four different orifices without chamfered edges and having β ratios of 0.66, 0.72, 0.77 and 0.83 were used to carry out the CCF slugging experiments. The experiments were repeated by changing the position of the orifices with respect to the elbow in the horizontal leg; these positions are indicated as Position 1 and Position 2 in Fig. 1. Furthermore, experiments were also carried out without orifices installed in the horizontal leg. The data have been treated in order to obtain the onset of flooding and slugging, the slug propagation velocity, the slug frequency, and the average void fraction as a function of both the liquid and gas superficial velocities.

4.1. Onset of flooding and onset of slugging

Collected data on the onset of flooding and slugging as a function of the liquid and gas superficial velocities are shown in the Fig. 5(a) and (b). Note that dark symbols are used to identify the flooding data while slugging data are identified by using white symbols. As can be observed, with

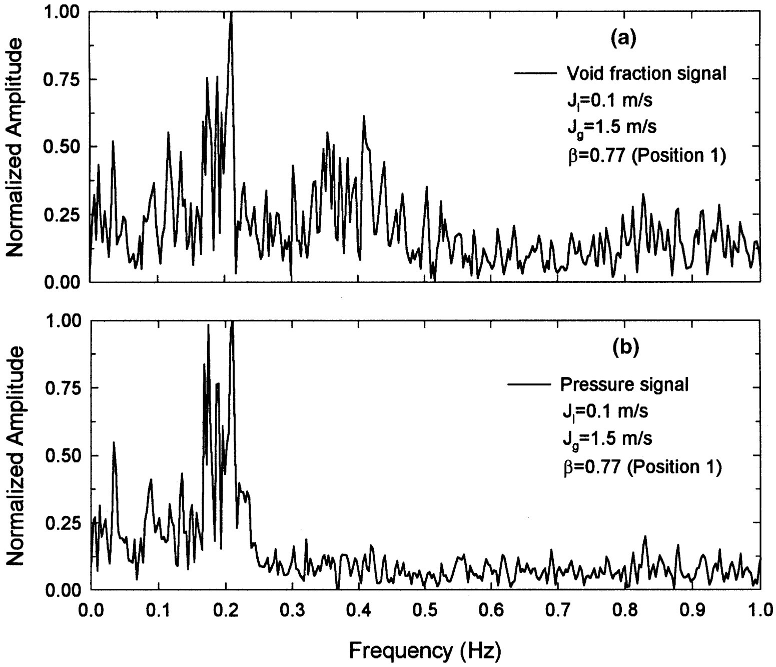

Fig. 4. Typical power spectra of void fraction and pressure signals.

the exception of the experiments carried out without an orifice (Fig. 5(c)), the points that correspond to the onset of flooding and slugging seem to be quite close. Thus, when an orifice is installed in the horizontal leg, and for the conditions used during the present experiments (both the liquid and the gas superficial velocities are kept constant for each experiment), flooding is simultaneously accompanied by the formation of slugs in the horizontal leg. Siddiqui et al. (1986) and Kawaji et al. (1991) have observed that at high superficial liquid velocities a hydraulic jump formed in the horizontal leg close to the elbow and that flooding was caused by slugging which simultaneously occurred at this point. Fig. 5(a) and (b) also show that for a constant value of the superficial gas velocity, the required superficial liquid velocity necessary to provoke flooding and/or slugging decreases by increasing severity of the obstruction.

It has been visually observed that once flooding is triggered, a pulsating column is simultaneously formed in the vertical leg. This pulsating column, under the same onset of flooding flow conditions, subsequently triggers the formation of high amplitude waves that travel along the horizontal leg toward the orifice. Fig. 6 shows a schematic representation of these phenomena. The waves that are formed close to the elbow and propagate downstream in the horizontal leg are then partially reflected by the orifice. Fig. 7(a) shows a photo of a wave, produced by the pulsating column, traveling downstream toward the orifice. It is interesting to note the undular bord shape of this wave (Johnson, 1997). These waves travel along the horizontal leg and depending on the orifice size a partial reflection occurs at the orifice. Fig. 7(b) shows a photo of two waves traveling in opposite directions, with the reflected wave produced by an orifice located at Position 1 in the horizontal leg. Each time an incident wave produces a constructive interference with a reflected one, and the resulting amplitude becomes equal to the tube ID blocking the passage of the gas, a slug

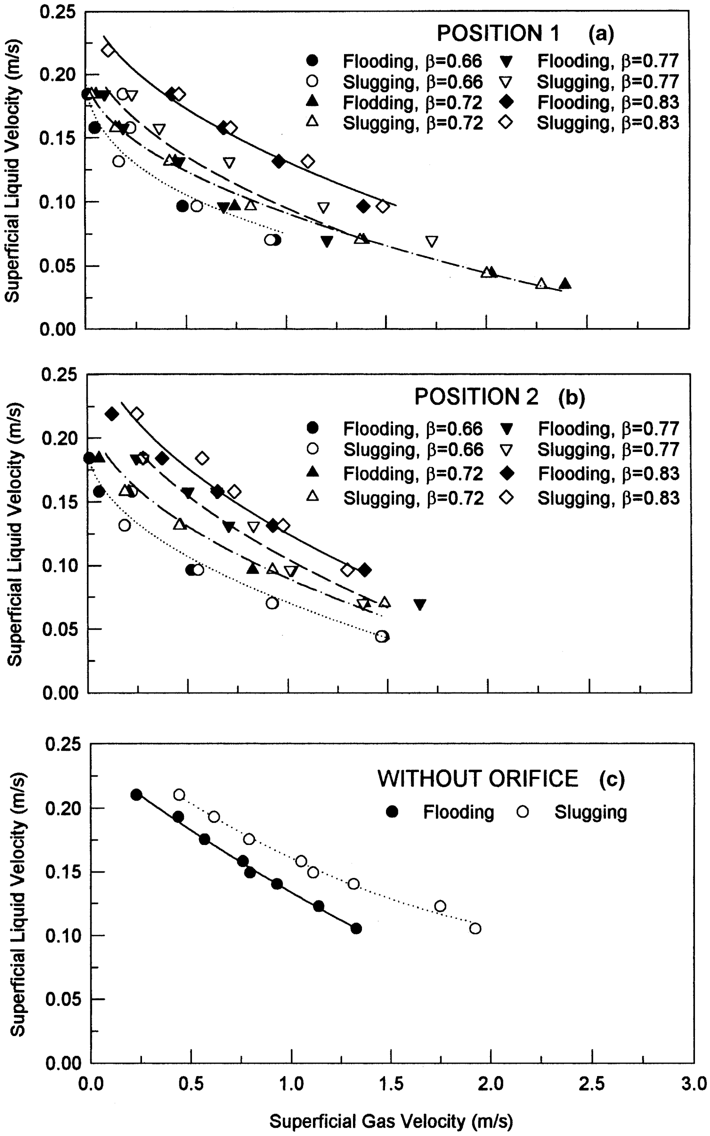

Fig. 5. Flooding and slugging conditions vs. the superficial gas velocity.

of liquid is formed. It is obvious that the probability of a constructive interaction between these waves will depend on their amplitudes; thus, the greater the severity of the obstruction the higher will be the amplitude of the reflected waves. This may explain the fact that for a constant superficial liquid velocity the superficial gas velocity necessary to form the slugs decreases as the severity of the obstruction increases. These waves, and consequently the interaction between the incident and reflected ones maintain the formation of slugs over almost the entire liquid delivery region. Approaching zero liquid penetration conditions, the thickness of the liquid film is considerably reduced, diminishing the propagation of high amplitude waves up to a point where the formation

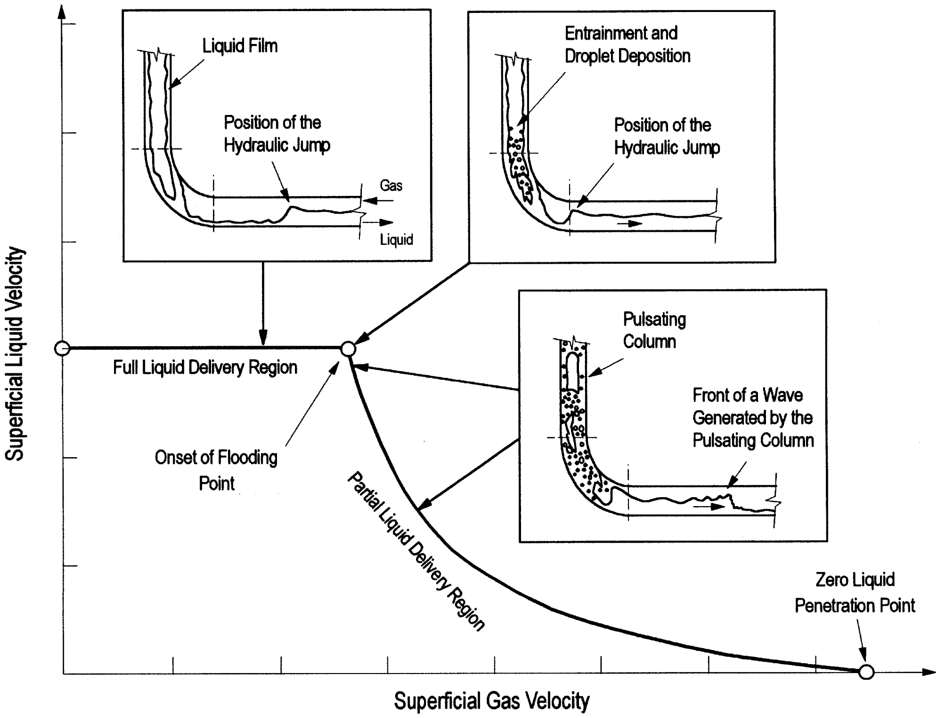

Fig. 6. Schematic representation of the wave formation phenomena.

of slugs completely disappears. It is important to mention that some of the experimental points do not appear in Fig. 5(a) and (b) because they are hidden by points corresponding to the same values of superficial velocities.

A comparison of Fig. 5(a) and (b) shows that both, the onset of flooding and the onset of slugging seem to be independent of the location of the orifice with respect to the elbow. This observation confirms that at least for the experimental conditions covered during these experiments, the onset of flooding and slugging are mostly controlled by hydrodynamic effects taking place close to the elbow. Similarly to Siddiqui et al. (1986) and Kawaji et al. (1993), before flooding starts taking place, the formation of a hydraulic jump close to the elbow has been observed. When the gas flow rate is subsequently increased, the hydraulic jumps moves toward the elbow and flooding occurs immediately after the hydraulic jump disappears inside the elbow (see Fig. 6). Wan and Krishnan (1986) and Siddiqui et al. (1986), for low superficial liquid velocities in a horizontal test section, observed that flooding occurred when the hydraulic jump was dragged towards the elbow. Kawaji et al. (1991), however, observed that for moderate superficial liquid velocities, the location of the hydraulic jump is pushed towards the exit of the horizontal pipe, away from the elbow. Under such a condition they observed that the flooding mechanism changes to slugging occurring close to the end of the horizontal pipe.

For the experiments carried out without an orifice installed in the horizontal leg a difference between flooding and slugging conditions is observed (Fig. 5(c)). Similarly to the experiments carried out with an orifice installed in the horizontal leg, the onset of flooding is accompanied by the

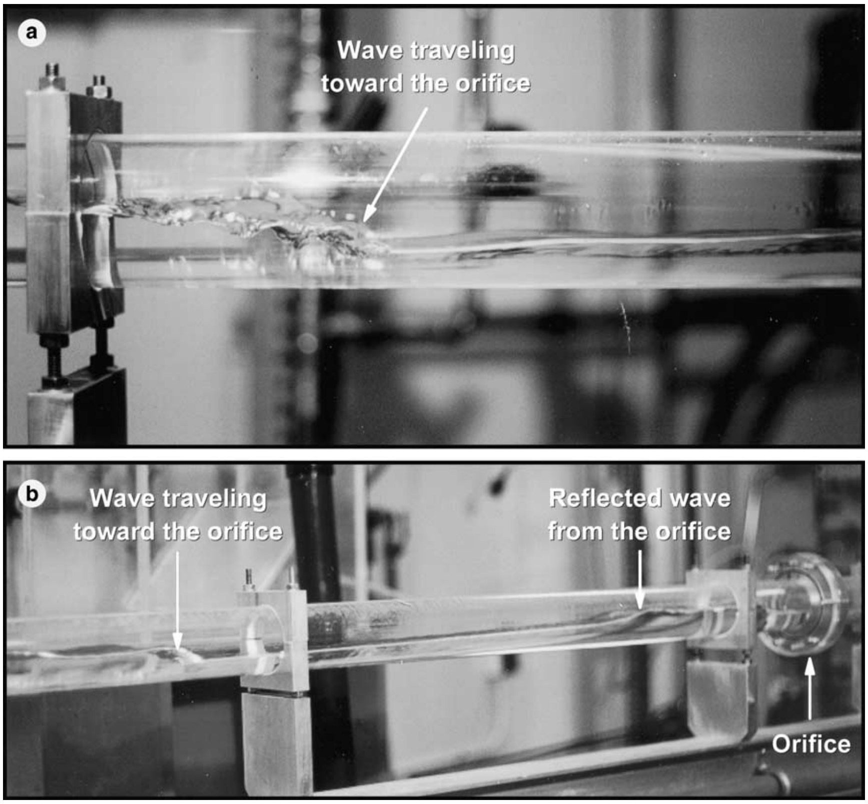

Fig. 7. (a) Wave produced by the pulsating column. (b) Incident and reflected waves.

formation of a pulsating column in the vertical leg. The waves produced by the pulsating column now travel downstream to the second elbow located close to the lower plenum (see Fig. 1). Due to the distance that separates the two elbows, the reflected waves from the second elbow are in general of very low amplitude. Diminishing the amplitude of the incident and reflected waves prevents a constructive interference having the required amplitude for the bridging of the pipe to occur. By increasing the superficial gas velocity above that required to produce flooding, it is observed however, that two different kinds of slugs start forming in the horizontal leg. The first kind are very short ones that form close to or even inside the first elbow. The second kind of slugs are very long ones (occupying almost 2/3 of the horizontal leg) which are formed immediately upstream of the second elbow (close to the lower plenum). Therefore, it is apparent that the hydrodynamic mechanisms that control the formation of the slugs when an orifice is installed in the horizontal leg are different when there is no orifice installed in the horizontal leg.

4.2. Slug propagation velocity

As has been mentioned in the experimental conditions and procedures section, the slug propagation velocities were determined by cross-correlating the signals produced by the slug detection probes in conjunction with the distance between these probes. For the present experiments, three probes were placed at different locations between the elbow and the first flange used to install the orifice (Position 1 in Fig. 1). Due to the extent of the slugs observed in some experiments and to the formation of a highly perturbed region close to the elbow in other cases, the position of the probes with respect to the elbow, as well as the distances between the probes were not the same for all the experiments. The following distances between the probes were used during the experiments: 0.20, 0.35, and 0.40 m while the distance of the first probe with respect to the elbow was maintained constant at 0.19 m. Due to the thickness of the probes (Teyssedou and Tye, 1999) it is quite difficult if not impossible to determine the effective distance between them. In all the cases it has been considered that this distance cannot be determine with an accuracy better than ± half of the thickness of a probe, i.e., 12 mm.

Fig. 8(a) shows the time record of the liquid hold-up obtained from a typical void fraction signal collected for an experiment carried out with an orifice having a β ratio of 0.83. At least three slugs separated by ≈4 s each can be easily identified in this figure, where the following key aspects can be observed:

(a) the slugs are formed just behind waves propagating downstream from the elbow, note that these waves are characterized by moderate amplitudes and relatively low frequencies,
(b) the void fraction in the slug front tends to increase substantially,
(c) in the body of the slug the void fraction does net reach a zero value, i.e., full liquid hold-up,
(d) the slug tail is characterized by the highest void fraction and
(e) the slug tail is characterized by high frequency low amplitude waves.

The presence of high amplitude, low frequency waves just before the slugs start forming agrees with the observation that the slugs are caused by the constructive interaction of high amplitude waves traveling in opposite directions. A schematics of a typical slug is shown in Fig. 9. The high void content observed in the slug front is due to an important quantity of air trapped by the slugs during their formation. Furthermore, this air content, even though it diminishes significantly after the slug is formed, does not completely disappear from the body of the slug. As can be observed in Fig. 8(a), the air trapped in the slug body limits the maximum liquid hold-up. The formation of a slug behaves as a blockage for the liquid phase, thus the content of liquid in the slug tail is substantially reduced, which explain the fact that the void content in this region increases up to a maximum value (for the case shown in the Fig. 8(a) the void fraction in this region is close to 80%). The acceleration and subsequent deceleration of the gas phase in this region, characterized by a small liquid film thickness (high void fraction) in conjunction with the gas–liquid interfacial drag, may explain the formation of the small amplitude high frequency waves observed. Fig. 8(b) and (c) show the void fraction records obtained from experiments carried out under similar flow conditions with orifices having β ratios of 0.66 and 0.83 respectively, located at Position 1 in the horizontal leg. From these figures it can be observed that for the lower β ratio (=0.66) the time interval between the slugs is shorter than that observed for the higher β ratio (=0.83). Furthermore, lower β ratios seem to produce much shorter slugs which are characterized by a much higher void content than those observed for a higher β ratio (compare the value of the void fraction reached by the lowest peaks in these figures).

The data on the slug propagation velocity as a function of the superficial gas velocity, obtained with orifices having different β ratios installed at both axial positions in the horizontal

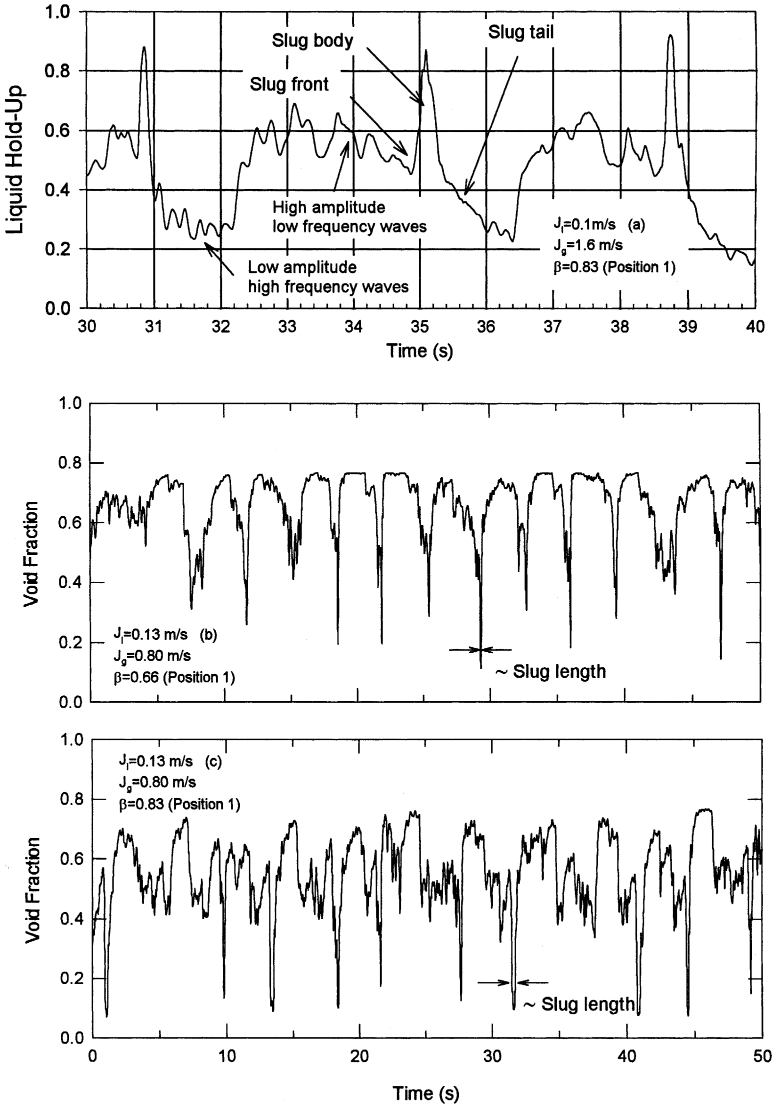

Fig. 8. Time records of: (a) liquid hold-up and (b,c) void fraction signals.

leg (Positions 1 and 2 in Fig. 1) are shown in Fig. 10. For the range of the experimental conditions used to carry-out the experiments, it is in general observed that the slug propagation velocity does not depend on either the orifice's size or the position of the orifice with respect to the elbow. It is also observed that the superficial liquid velocity does not affect the slug propagation velocity (Note that the data presented in Fig. 10 cover the full range of superficial liquid velocities, from the onset of slugging up to the zero liquid penetration point). Further, the slug propagation velocity decreases, almost linearly with the superficial gas velocity. The same figure shows the best fit of the data by using a simple linear regression curve given by, $V_s = 0.821 - 0.151 J_g$.

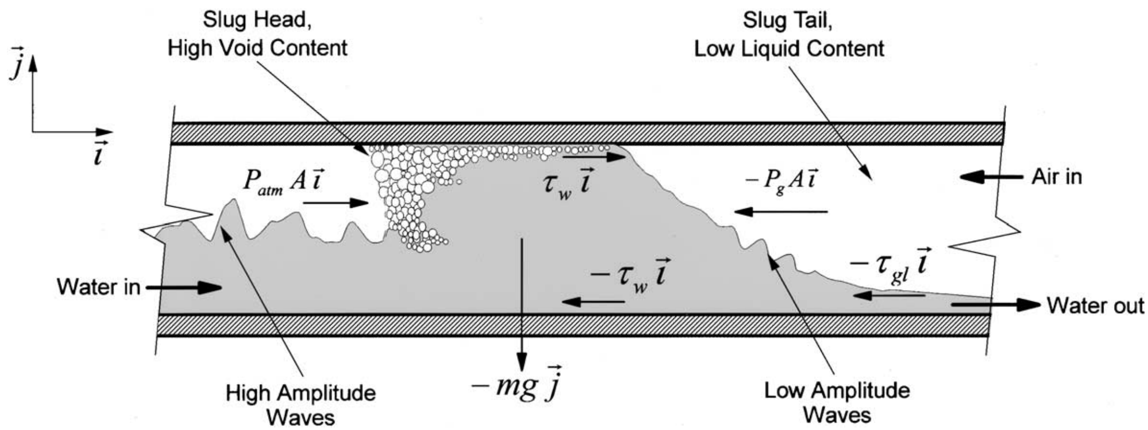

Fig. 9. Schematic and forces acting on a typical slug.

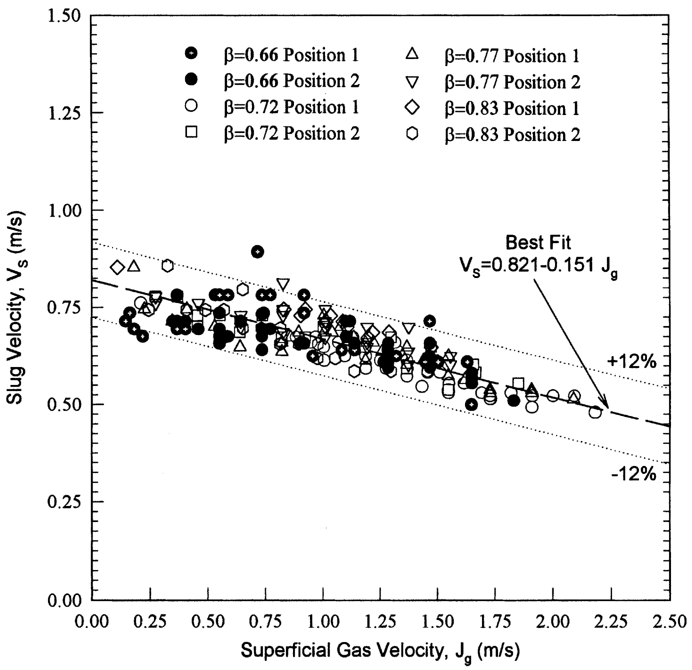

Fig. 10. Slug velocity vs. superficial gas velocity for all orifice β ratios and positions.

A balance of forces caused by pressure, i.e., neglecting factional forces between the slug and the pipe, taken on a typical slug shows that the driving force that keeps the slug moving is a function of the pressure difference across the slug head and tail (see Fig. 9). Assuming the atmospheric pressure P_{atm} acting on the slug head, then the slug movement must be controlled by the effective pressure exerted by the air on its tail, P_g. In turn, this pressure is equal to the gas pressure at the lower plenum (see Fig. 1) minus the pressure drop essentially due to the interfacial drag at the liquid–gas interface. At this point, it is important to consider the fact that during the whole slugging process, a non-negligible amount of liquid is still delivered (the region before reaching the zero liquid penetration point in Fig. 6). This liquid flows downstream towards the lower plenum, passing across the orifice which fixes its height in this region, i.e., liquid content in the slug tail. Furthermore, in the slug tail region, the interfacial friction depends on the relative velocity of the two phases flowing counter-currently. Data collected by Bédard (1997) for the entire partial liquid delivery region up to the zero liquid penetration point and using the same experimental facility, was used to evaluate the product of the interfacial area per unit length and the square of the relative velocities between the phases. The results obtained with an orifice located at Position 1 and Position 2 are shown in Fig. 11. It is apparent that this product, which should control the interfacial drag and consequently the driving force applied to the slug, increases with increasing superficial gas velocity. Orifices having β ratios of 0.66, 0.72 and 0.77 are characterized by almost the same interfacial drag. However, for $\beta = 0.83$ a huge difference is observed for superficial gas velocities lower than 1.5 m/s. There are two possible reasons that can explain this departure. First, it is important to mention that these conditions (i.e., higher β ratios and low superficial gas velocities) correspond to the highest superficial liquid velocities applied during the experiments thus, the delivered liquid flow rate was much higher and consequently the collection method used

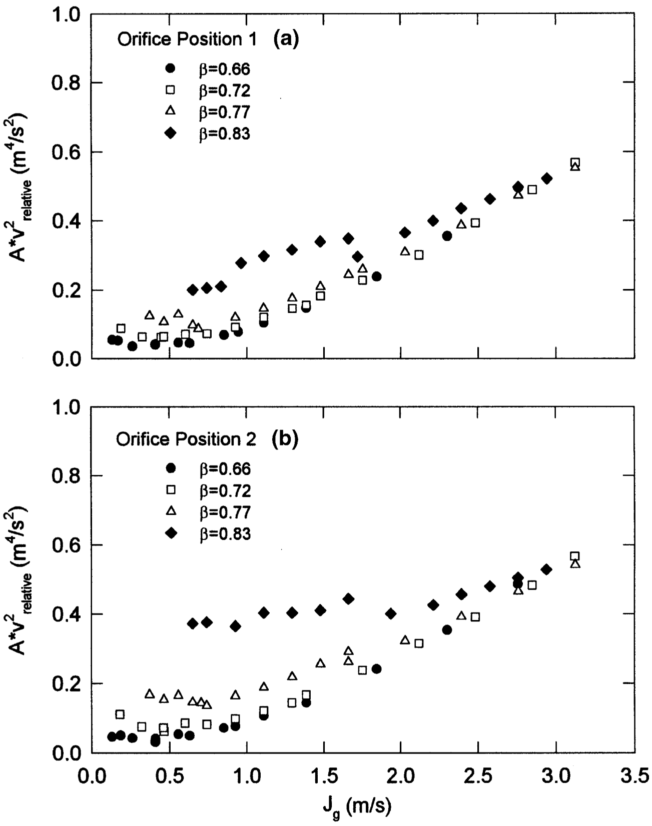

Fig. 11. Interfacial drag term.

was less accurate. Even though a systematic error introduced in the liquid collection procedure can explain the jump observed for a superficial gas velocity close to 1.5 m/s, it cannot entirely explain the results presented in Fig. 11. It is important to mention that the interfacial area per unit length (A in Fig. 11) as well as the cross-sectional areas occupied by the phases are calculated based on the liquid height that corresponds to the maximum value required for a given orifice to allow the liquid to pass through. For higher β ratios, however, the interfacial area calculated in this way as well as the cross-sectional area occupied by each phase becomes unrealistic; thus, the results presented in Fig. 11 must be considered only as qualitative. In general, Fig. 11 can be used to show the fact that the drag force exerted by the liquid on the gas phase in the slug tail region, increases with increasing superficial gas velocity. Consequently, increasing the superficial gas velocity, increases the interfacial friction pressure losses, that in turn reduces the effective driving force applied to the slug. The same figure also shows that the interfacial drag force seems to be almost independent of the orifice size and its position in the horizontal leg. This observation can be used to explain the fact that for a given superficial gas velocity a unique slug propagation velocity, independent of the orifice size and position is observed in Fig. 10. In addition, an increase in the gas pressure loss reduces the driving force acting on the slug; thus, the slug propagation velocity must decrease with increasing superficial gas velocity as shown in Fig. 10. It is important to mention that similar trends were observed by Jepson and Taylor (1993) for higher superficial gas velocities in co-current two-phase flows.

4.3. Slug frequency

As has been described above, in order to determine the slug frequency as a function of the gas and liquid superficial velocities, for each orifice size and position with respect to the elbow, the signals produced by the electrodes are post processed using autocorrelation and FFT. The normalized spectra obtained after treating the signals are analyzed and the first highest peak encountered within each spectral record is considered as the predominant frequency of the slugs. The capability of the hardware and software used to collect and treat the data was determined using the technique described in the experimental conditions and procedure section. It is important to remark that for very low frequencies and for some limited cases the first peak obtained from the FFT also corresponded to the same frequency determined by timing the formation of the slugs using a chronometer.

Fig. 12 shows the predominant slug frequency data as well as their best fits as a function of the gas superficial velocity obtained for the experiments carried out without orifices and with orifices having β ratios of 0.66, 0.72, 0.77 and 0.83 installed at Position 1 and Position 2 in the horizontal leg. In general it is observed that for both positions and for all the orifices tested, the predominant frequency decreases with increasing superficial gas velocity. It can also be seen that for a given superficial gas velocity and for a given orifice β ratio the frequency of the slugs is much higher when the orifice is located closer to the elbow, i.e., Position 1 in Fig. 1. Furthermore, the predominant slug frequencies are seen to increase with decreasing orifice β ratios.

As was described before, it was observed that the slugs are formed by a constructive interaction (interference) between waves that propagate in opposite directions. Large amplitude waves are generated by a pulsating column that forms above the elbow after reaching the onset of flooding condition (see Figs. 6 and 7). These waves are partially reflected by the orifice; thus, the mutual

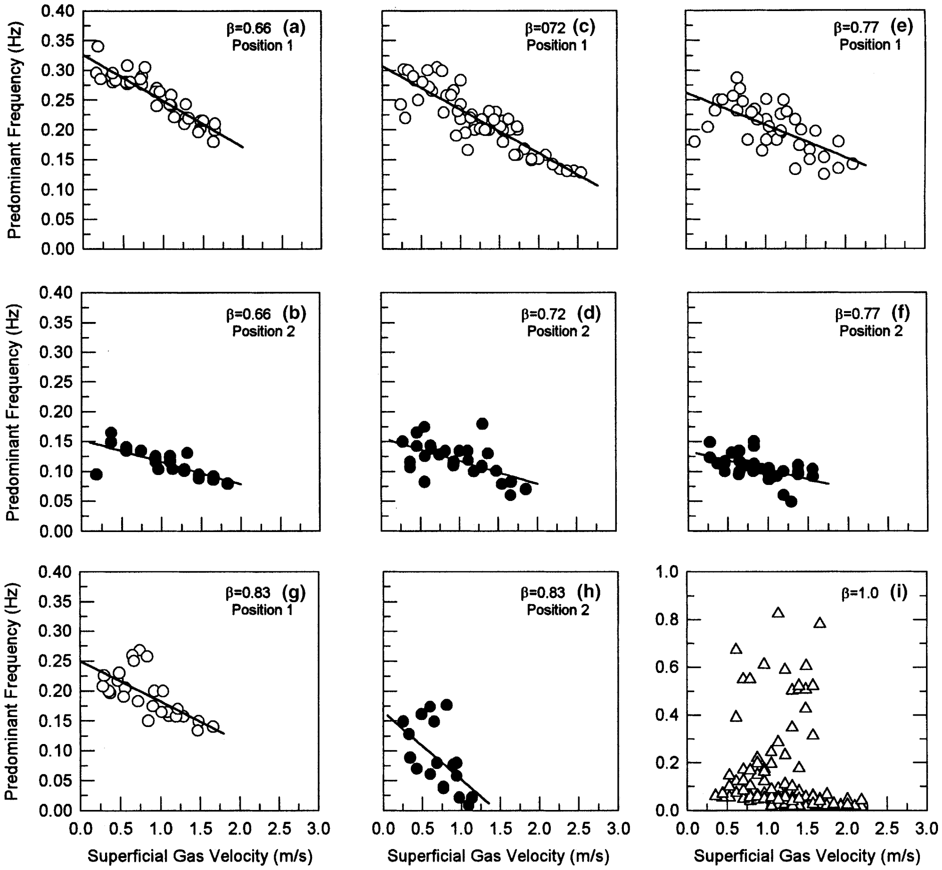

Fig. 12. Predominant slug frequency vs. superficial gas velocity.

interaction of the incident and the reflected waves brings about the bridging of the pipe. This type of wave interaction can explain the fact that the predominant frequency decreases both with increasing superficial gas velocity and the size of the orifice. For similar flow conditions a comparison of Fig. 8(b) and (c) show that the predominant slug frequency tends to decrease with increasing β ratio. For the same time record, the peaks that characterize the slugs are more spread out for $\beta = 0.83$ than for $\beta = 0.66$. The increase in the superficial gas velocity increases the amount of entrained liquid, thus reducing the water level in the pipe. In turn, the increase in the orifice size decreases the probability that the waves will be reflected. As the incident waves travel along the horizontal leg their amplitude gradually decreases, thus when the orifice is located farther away from the elbow the probability of the incident and reflected waves of bridging the pipe decreases, resulting in a lower slugging frequency.

Fig. 12(i) shows the predominant slug frequency for the experiments carried out without orifice ($\beta = 1.0$). It is interested to distinguish two different regions in this figure. The first region, where most of the data are concentrated, shows a quite low frequency that decreases with increasing superficial gas velocity. These data points correspond to quite long slugs that form at the second elbow located closer to the lower plenum (see Fig. 1). It is apparent that the slug frequencies in this region are in agreement with those observed for the orifice having the highest β ratio (=0.83). The second region, characterized by a huge scattering in the data, corresponds to very short, high frequency, slugs that are formed closer to or even inside the first elbow (Fig. 1). As has been mentioned before, most of these slugs were detected by one of the void probes that was kept at a constant and short distance from this elbow.

It must be pointed out that in the open literature, there is no available slug frequency data that have been collected for vertical-to-horizontal counter-current flow with orifices installed in the horizontal leg. To the best of the authors' knowledge, most of the existing studies are concerned with slugging in co-current two-phase flows. A comparison of the present results with the data presented for co-current flows in Dukler and Hubbard (1975), for superficial gas velocities lower than 2 m/s, shows a similar trend, i.e., the slug frequency decreases with increasing superficial gas velocity. For superficial gas velocities higher than 2 m/s, however, their data shows that the slug frequency increases at a very low pace with increasing J_g. It is important to remark, that the slug frequencies obtained during the present work are much lower than those obtained by Dukler and Hubbard. Several reasons can explain this difference; Dukler and Hubbard used a much smaller tube ID, they applied much higher superficial liquid velocities and the experiments were carried out under co-current flow conditions. In a similar study, Jepson and Taylor (1993) have shown that increasing the tube inside diameter decreases the slug frequency, because a higher inside diameter decreases the probability of a wave of bridging the tube (Please note that Jepson and Taylor carried out the experiments for co-current flows at a much higher superficial velocities than those used in the present work, i.e., $2 < J_g < 14$ m/s).

4.4. Average void fractions

Fig. 13 shows the average void fraction as a function of the superficial gas velocity for all the cases studied. The same figure also shows the regression lines of the data. With the exception of the experiments carried out without orifice (Fig. 13(i)), it can be observed that for superficial gas velocities higher than 0.5 m/s an almost unique asymptotic value of the average void fraction close to 80% is reached. This asymptotic value seems to be independent of the size of the orifice and its position with respect to the elbow. This constant value can be explained by a complex relationship of slug frequency, slug length and slug void content. As a matter of fact, it has been observed that for a given superficial gas velocity, the lower the β ratio the lower the slug frequency. In addition, orifices having small β ratios produce shorter slugs with a much higher void content (see Fig. 8(b) and (c)). The relationship between these factors results in a time average void fraction which is almost constant for all the orifices tested during the present study. For superficial gas velocities lower than 0.5 m/s, it has been observed that both the frequency of the slugs and the length of the slugs increases. In general, very low superficial gas velocities correspond to quite high superficial liquid velocities (Bédard, 1997) which in turn provoke the formation of quite long slugs. It must be pointed out that during this work the slug lengths were not measured; thus, the aforementioned analysis is based on visual observations of the phenomena (the experiments were recorded with a digital video camera that allowed us to view the experiments in slew motion, reducing in this way any "subjective" appreciation of some of the features described in the paper).

Fig. 13(i) shows the average void fraction obtained for the experiments carried out without an orifice. In general, a huge scattering in the data is observed, further the asymptotic value (if there

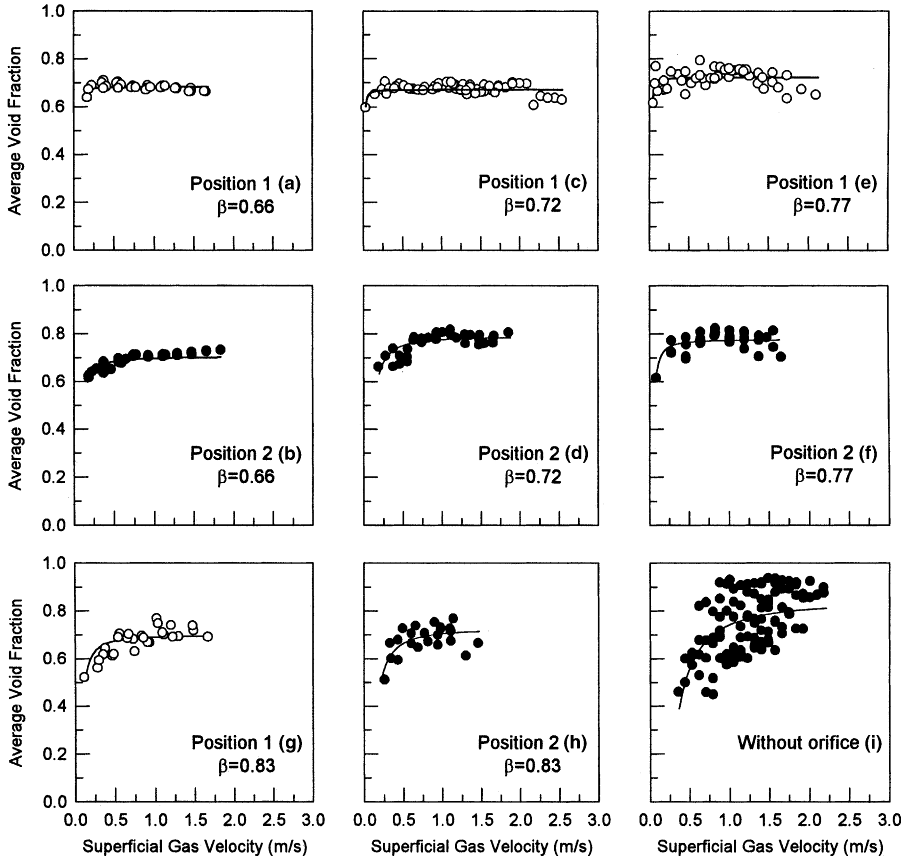

Fig. 13. Average void fraction vs. the superficial gas velocity.

is any) seems to be slightly higher than that observed for the experiments carried out with an orifice installed in the horizontal leg. It is important to mention that the scattering in the data is due to the fact that, as has been mentioned before, two different types of slugs are formed when there is no orifice installed in the pipe; very long slugs generated closer to the second elbow and very fast shorter ones formed quite close to the first elbow. The fact that high frequency shorter slugs can trap more gas, may explain the higher average void fraction observed for this case ($\beta = 1.0$). It is important to note that similar trends were observed by Wallis and Dobson (1973) and Woods and Hanratty (1996) who conducted the experiments in a 0.095 m ID, 26.5 m long pipe with air and water flowing co-currently. Moreover, Wallis and Dobson found that the void fraction was also independent of the superficial liquid velocity as has been observed in the present work.

5. Conclusions

Experimental counter-current flow data on the onset of flooding and slugging, the slug propagation velocity, the predominant slug frequency and the average void fraction have been obtained by using different size orifices installed at two locations in a horizontal pipe. For the flow conditions covered during these experiments, it has been observed that there is no significant difference between the onset of flooding and the onset of slugging when an orifice is installed in the horizontal run. However, a difference has been observed for the experiments carried out without orifices. Furthermore, the position of the orifice does not affect the onset of flooding and slugging.

The visual observations carried out during the experiments have shown that when an orifice is installed in the horizontal leg, slugs occur due to the mutual interaction (constructive interference) of two waves traveling in opposite directions. This means that a completely different mechanism seems to govern the formation of slugs in counter-current two-phase flows in horizontal partially blocked channels. This is in contrast to that described for the slugging phenomena in co-current flow, where wave instability seems to be the principal mechanisms responsible of bridging the pipe.

The analysis of the data has shown that for a fixed superficial liquid velocity an increase in the superficial gas velocity causes a decrease in both the slug propagation velocity and the slug predominant frequency. A possible explanation has been given as: an increase in superficial gas velocity causes an increase in the amount of liquid entrainment which reduces the height of the liquid in the horizontal leg, decreasing the probability of constructive interaction between the waves. Furthermore, a decrease in the frequency is observed in both cases; either increasing the size of the orifices or placing the orifices further away from the elbow. However, there are no such significant effects of size and position with respect to the elbow on the slug propagation velocity. A justification of this observation has been given based on the interfacial drag force that has been shown to increase with increasing superficial gas velocity. Further, for high superficial gas velocities a unique asymptotic value of the average void fraction was determined. This value seems to be independent of both the orifice size and its location with respect to the elbow. For the experiments carried out without an orifice it was found that two different kinds of slugs are formed. High frequency and quite short slugs formed immediately downstream of the first elbow while very long slugs were observed to be formed closer to the second elbow near the lower plenum.

To the best of the authors' knowledge, this is the first study on slugging phenomena for counter-current vertical-to-horizontal flows with orifices installed in a horizontal pipe. Therefore, there is no available data in the open literature on slugging phenomena for counter-current two phase flows to be compared with.

Acknowledgements

This work has been partially funded by the Natural Science and Engineering Research Council of Canada (NSERC) under the individual grant #OGP0041929, the Hydro-Québec Chair in Nuclear Engineering and the CANDU Owners Group (COG).

References

Ardron, K.H., Banerjee, S., 1986. Flooding in an elbow between a vertical and horizontal or near-horizontal pipe. Part II: Theory. Int. J. Multiphase Flow 12, 543–558.

Bankoff, S.G., Lee, S.C., 1986. A critical review of the flooding literature. In: Hewitt, G.F., Delhaye, J.M., Zuber, N. (Eds.), Multiphase Science and Technology, vol. 2. Hemisphere, New York (Chapter 2).

Bédard, S., 1997. Effet de la position d'une obstruction par rapport à un coude dans un écoulement diphasique contre-courant. Master's Thesis. École Polytechnique, Montréal.

Celata, G.P., Cumo, N., Farello, G.E., Setaro, T., 1989. The influence of flow obstructions on the flooding phenomena in vertical channels. Int. J. Multiphase Flow, 227–239.

Crowley, C.J., Wallis, G.B., Barry, J.J., 1992. Validation of a one-dimensional wave model for the stratified-to-slug flow regime transition, with consequences for wave growth and slug frequency. Int. J. Multiphase Flow 18, 249–271.

Dukler, A.E., Hubbard, M.G., 1975. A model for gas–liquid slug flow in horizontal and near horizontal tubes. Ind. Eng. Chem. Fund. 14, 337–347.

Jepson, W.P., Taylor, R.E., 1993. Slug flow and its transitions in large diameter horizontal pipes. Int. J. Multiphase Flow 19, 411–420.

Johnson, R.S., 1997. A modern introduction to the mathematical theory of water waves. Cambridge Texts in Applied Mathematics. Cambridge University Press, pp. 374 (Chapter 5).

Johnston, A.J., 1985. Transition from stratified to slug regime in counter-current flow. Int. J. Multiphase Flow 11, 31–41.

Kawaji, M., Thomson, L.A., Krishnan, V.S., 1989. Analysis of countercurrent flooding in vertical-to-inclined pipes containing elbows of varying angle. CNS 15th Annual Reactor Simul. Symp., Massasauga, Ontario.

Kawaji, M., Thomson, L.A., Krishnan, V.S., 1991. Countercurrent flooding in vertical to-inclined pipes. Exp. Heat Transfer 4, 95–110.

Kawaji, M., Lotocki, P., Krishnan, V.S., 1993. Countercurrent flooding in pipes containing multiple elbows and an orifice. JSME Int. J., Ser. B 36, 95–110.

Krowlewski, S.M., 1980. Flooding in a simulated nuclear reactor hot leg. Bachelor's Thesis. MIT.

Siddiqui, H., Ardron, K.H., Banerjee, S., 1986. Flooding in an elbow between a vertical and horizontal or near horizontal pipe. Part I: Experiments. Int. J. Multiphase Flow 12, 531–541.

Taitel, Y., Dukler, A.E., 1976. A theoretical approach to the Lockhart Martinelli correlation for stratified flow. Int. J. Multiphase Flow 2, 591–595.

Taitel, Y., Dukler, A.E., 1977. A model for slug frequency during gas–liquid flow in horizontal and near horizontal pipes. Int. J. Multiphase Flow 3, 585–596.

Teyssedou, A., Tye, P., 1999. A capacitive two-phase flow slug detection system. Rev. Sci. Instrum. 70, 3942–3948.

Tien, C.L., Chung, K.S., Liu, C.P., 1979. Flooding in two-phase countercurrent flows. EPRI Report NP-1283.

Tye, P., 1997. Counter-current flow and flooding in vertical and horizontal tubes with and without obstructions. Ph.D. Thesis. École Polytechnique, Montréal.

Tye, P., Teyssedou, A., 2000. Adiabatic counter-current flow in channels containing singularities. Final Report, WPIR-1513, COG-99-238.

Wallis, G.B., Dobson, J.E., 1973. The onset of slugging in horizontal stratified air–water flow. Int. J. Multiphase Flow 1, 173–193.

Wan, P.T., Krishnan, V.S., 1986. Air–water flooding in a 90° elbow with a slightly inclined leg. 7th Ann. Conf. CNS, Toronto.

Woods, B.D., Hanratty, T.J., 1996. Relation of slug stability to shedding rate. Int. J. Multiphase Flow 22, 809–828.